Translational Oncology
www.transonc.com

Volume 7 Number 3 June 2014 pp. 393–399 393

Low-Dose Vascular Photodynamic Therapy Decreases Tumor Interstitial Fluid Pressure, which Promotes Liposomal Doxorubicin Distribution in a Murine Sarcoma Metastasis Model[1]

Jean Yannis Perentes*, Yabo Wang*, Xingyu Wang*, Etienne Abdelnour*, Michel Gonzalez*, Laurent Decosterd†, Georges Wagnieres‡, Hubert van den Bergh‡, Solange Peters§, Hans-Beat Ris* and Thorsten Krueger*

*Division of Thoracic and Vascular Surgery, Centre Hospitalier Universitaire Vaudois, Lausanne, Switzerland; †Department of Clinical Pharmacology and Toxicology, Centre Hospitalier Universitaire Vaudois, Lausanne, Switzerland; ‡Laboratory of Organometallic and Medicinal Chemistry, Ecole Polytechnique Federale de Lausanne (EPFL), Lausanne, Switzerland; §Department of Oncology, Centre Hospitalier Universitaire Vaudois, Lausanne, Switzerland

Abstract

INTRODUCTION: Solid tumors are known to have an abnormal vasculature that limits the distribution of chemotherapy. We have recently shown that tumor vessel modulation by low-dose photodynamic therapy (L-PDT) could improve the uptake of macromolecular chemotherapeutic agents such as liposomal doxorubicin (Liporubicin) administered subsequently. However, how this occurs is unknown. Convection, the main mechanism for drug transport between the intravascular and extravascular spaces, is mostly related to interstitial fluid pressure (IFP) and tumor blood flow (TBF). Here, we determined the changes of tumor and surrounding lung IFP and TBF before, during, and after vascular L-PDT. We also evaluated the effect of these changes on the distribution of Liporubicin administered intravenously (IV) in a lung sarcoma metastasis model. *MATERIALS AND METHODS:* A syngeneic methylcholanthrene-induced sarcoma cell line was implanted subpleurally in the lung of Fischer rats. Tumor/surrounding lung IFP and TBF changes induced by L-PDT were determined using the wick-in-needle technique and laser Doppler flowmetry, respectively. The spatial distribution of Liporubicin in tumor and lung tissues following IV drug administration was then assessed in L-PDT–pretreated animals and controls (no L-PDT) by epifluorescence microscopy. *RESULTS:* L-PDT significantly decreased tumor but not lung IFP compared to controls (no L-PDT) without affecting TBF. These conditions were associated with a significant improvement in Liporubicin distribution in tumor tissues compared to controls ($P < .05$). *DISCUSSION:* L-PDT specifically enhanced convection in blood vessels of tumor but not of normal lung tissue, which was associated with a significant improvement of Liporubicin distribution in tumors compared to controls.

Translational Oncology (2014) 7, 393–399

Introduction

The efficacy of drug therapy is partly related to the ability of the therapeutic agent to reach its target. The delivery of chemotherapeutics to tumors was shown to be influenced by the tumor blood supply, the drug transport through the vascular wall, and the drug diffusion/convection through the interstitial space [1,2]. Various methods have been tested to improve drug distribution, including isolated organ

Address all correspondence to: Jean Yannis Perentes MD-PhD, Division of Thoracic and Vascular Surgery, Centre Hospitalier Universitaire Vaudois, Rue du Bugnon 46, 1011 Lausanne, Switzerland. E-mail: jean.perentes@chuv.ch

[1] Grants: Swiss National Foundation grant (320030–135197 to H.-B.R.); Faculty of Biology and Medicine, University of Lausanne grant (to J.Y.P.); Swiss Society of Surgery grant (to J.Y.P.); and Julia Jacobi Photomedicine grant (to X.W.).
Received 15 January 2014; Revised 24 March 2014; Accepted 26 March 2014

1936-5233/14
http://dx.doi.org/10.1016/j.tranon.2014.04.010

perfusion, drug physiochemical property changes, and tumor vessel modulation [3–5].

Photodynamic therapy was initially designed to destroy tumor cells and the tumor vasculature. It consists of the administration of a photosensitizer that, after activation by nonthermal light, produces a variety of changes at the cellular level in the treated area [6]. Recently, low-dose photodynamic therapy (L-PDT) was shown to enhance the extravasation of macromolecular compounds into tumors [7,8]. For example, vascular L-PDT of sarcoma metastasis in a murine model resulted in a significant and selective enhancement of liposomal doxorubicin (Liporubicin; Regulon Inc, Athens, Greece) in tumors. The enhanced drug penetration in tumors was observed with different modes of Liporubicin administration (IV and isolated lung perfusion). Similar results were found in a different murine model of colon cancer, lung adenocarcinoma, and mesothelioma [7–10]. However, the precise mechanism by which L-PDT improves drug transport through the tumor vasculature remains unknown.

For macromolecular drugs (<100 nm in diameter), it was recently demonstrated that convection is the main promoter of drug extravasation between the intravascular and extravascular spaces [11]. The latter is dependent on the Starling equation that includes two main parameters, namely, tumor hydrostatic and oncotic pressures. A hallmark of malignant cancer is the angiogenic switch that primarily occurs through vascular endothelial growth factor. High levels of vascular endothelial growth factor were shown to alter the tumor vascular organization, to increase vascular permeability and the interstitial fluid pressure (IFP) thus hindering convection and drug delivery [1,2,4]. Many methods have been suggested to improve drug uptake and selectivity in tumors among which is vasculature "normalization." The latter was shown to occur with low doses of antiangiogenic therapy given at appropriate intervals, which caused a transient decrease in tumor vascular permeability and IFP. This made the vessels function in a more "normal" way and improved convection and concomitant drug delivery to tumors [2,4].

In the present study, we hypothesized that L-PDT caused a transient improvement in the function of tumor vasculature in a somewhat similar way to "vascular normalization." In a rodent model of sarcoma metastasis, we studied the changes in tumor and lung tissue (IFP) as well as TBF before, during, and up to 1 hour after low-dose Visudyne (Novartis, Hettlingen, Switzerland)–mediated L-PDT. In parallel, the uptake of Liporubicin administered IV was determined by epifluorescent microscopy in tumor and lung tissues.

Material and Methods

Study Design

Thirty-eight Fischer rats (Charles River Laboratories, France) underwent subpleural sarcoma implantation in their left lower lobe. This was followed 10 days later by a re-thoracotomy. Tumor L-PDT was performed using Visudyne and laser light. This was directly followed by the administration of Liporubicin, which was allowed to circulate for 1 hour. IFP was measured in tumor and normal lung in 10 and 8 animals, respectively, before and during 1 hour following L-PDT. In a separate set of five animals, TBF was measured in tumors before and during 1 hour following L-PDT. Liporubicin concentration and distribution in tumors and surrounding lung were assessed by epifluorescence microscopy performed on samples embedded in a cryogenic gel (OCT; Electron Microscopy Sciences, Hatfield, PA, USA) in the different treatment groups (n = 5 per group, total = 10). Finally, five animals were used as controls with no L-PDT. In these, all procedures including Visudyne and Liporubicin were injected, but no light was delivered.

Animals and Housing

Male Fischer rats weighing 250 to 300 g were treated in accordance with the Animal Welfare Act and the National Institutes of Health "Guidelines for the Care and Use of Laboratory Animals" and according to the Local Ethical Committee of the University of Lausanne.

Tumor Cell Line

A syngeneic methylcholanthrene-induced sarcoma (MCA) cell line was used as previously described [3]. It was cultivated at 37°C with 5% CO_2 in 20 ml of Roswell Park Memorial Institute (RPMI) medium 1640 medium containing glutaril, 10% FBS, and 1% penicillin/streptomycin (Invitrogen Corporation/Gibco/Life Technologies Ltd, Paisley, United Kingdom).

Subpleural Tumor Generation in the Left Lower Lung Lobe

This procedure was performed as described previously [3]. Briefly, animals were anesthetized by pentobarbital sodium (50 mg/kg), and oro-tracheal intubation was performed using a 16-gauge polyethylene Angiocath (Becton Dickinson, Sandy, UT). Animals were ventilated with a mixture of oxygen and isofluran (0.5%-2%, Forene; Abbott, Zug, Switzerland) using a tidal volume of 10 ml/kg and a respiratory rate of 75 to 90/min. A left-sided minithoracotomy was performed through the seventh intercostal space, and 0.1 ml of MCA cell solution containing 5×10^7 viable tumor cells was injected subpleurally into the left lower lobe using a 27-gauge needle [12]. The thoracotomy was closed layer by layer, and the endotracheal tube was removed.

L-PDT of Lungs Bearing Sarcoma Metastasis

Treatment was initiated when the tumors had reached a size of approximately 4 to 6 mm in diameter (approximately 7 days) as previously described [13]. The animals were anesthetized, and a left-sided thoracotomy was performed through the fourth intercostal space. The left lung was freed from its adhesions. A left cervical incision was performed to cannulate the external jugular vein. Visudyne was dissolved in NaCl (0.9%) and glucose (5%) and injected at a dose of 0.0625 mg/kg. After 15 minutes, laser light was applied to the exposed lower lung at a wavelength of 689 nm by an optical fiber–based frontal light distributor (Medlight, Ecublens, Switzerland) coupled to a diode laser (4-W laser diode; Biolitec, Germany). Noncontact, nonthermal surface irradiation was performed to the tumor and the surrounding normal lung tissue with the incident laser beam directed perpendicular to the lung surface and centered on the tumor. The treatment spot had a diameter of 30 mm, and the treated area was exposed to an irradiance of 35 mW/cm^2 and a light dose of 10 J/cm^2 corresponding to a treatment time of approximately 5 minutes. The irradiances and the light doses were measured in real-time as previously described [7,12].

IV Administration of Liporubicin

Immediately after laser light delivery, 400 μg of Liporubicin dissolved in 0.5 ml of 6% Hydroxyethyl Starch (HAES) was injected through the external jugular vein catheter. The time interval between Liporubicin administration and harvesting of the left lung (Liporubicin circulation time) was 60 minutes. Control animals underwent exactly the same operative procedure (including Visudyne injection) but had no light therapy (no laser and kept in the dark) before Liporubicin administration.

IFP Determination

IFP in tumors and lung tissues was determined using the wick-in-needle technique [14]. Briefly, a custom-made 28-gauge needle with a 200-μm side hole located approximately 2 mm from the needle tip was coupled to a pressure sensor by a water column in polyethylene tubing (0.58-mm inner diameter), filled with heparinized water (70 U/ml). Three nylon sutures (7-0) were threaded through the needle to form the "wick." The signal from the pressure sensor was passed through an amplifier and digitalized (in a MacLab/4e AD Instrument Coorporation (Dunedin, New Zealand) converter). Data were collected using a Personnal Computer (PC) with PowerLab Chart software version 4.2 (ADInstruments Ltd). Before each experiment, the system was calibrated against a predefined height where the needle was submersed in a sterile water solution at tumor level (zero reference, heart level of the animal) and at a predefined elevation. A fresh, sharp needle was then introduced at the center of the tumor and in the subpleural parenchymal space of normal lung tissue in the L-PDT irradiation field but away from the tumor. Fluid communication between the tumor and the pressure transducer was checked by briefly clamping the tubing, hence causing a brief compression and decompression of the tube; when fluid communication was satisfactory, IFP quickly returned to the same value as before the clamping operation. The values were then allowed to stabilize and give the mean IFP. For lung IFP measurements, a change in the pressure measured that mirrored the ventilator suggested an intra-alveolar or intra-airway location of the needle. In this case, fluid communication was lost, and the needle was replaced in the lung parenchyma. Tests for adequate fluid communication were then repeated. L-PDT could be performed with the needle in place, and real-time evaluation of IFP could be determined. IFP was measured before, during, and at 10-minute intervals following L-PDT for up to 1 hour (time at which Liporubicin had circulated for 60 minutes and that the animals were killed). Every 10 minutes, fluid communication was checked by the clamping operation. At the end of the experiment, the needle was placed in sterile water, and calibration was checked to ensure no clogging of the needle had occurred.

Laser Doppler Flowmetry

TBF was determined by laser Doppler flowmetry perfusion measurement using a setup with a Periflux 4001 laser Doppler flowmeter (Perimed, Stockholm, Sweden) and a custom-built probe such as previously described [14]. Laser light at a wavelength of 780 nm was transmitted into the lung from the 42°C heated probe. The probe was held steady in the desired position by a micromanipulator. TBF was recorded continuously for 2 to 3 minutes, whereas the calculated perfusion in arbitrary perfusion units (PU) was monitored graphically. During recording, care was taken to position the probe such that respiratory movements did not influence the readings (this was determined from the graphic representation of measured PU values). As soon as steady state had been reached (typically in 60-90 seconds), three individual values were noted from the display. The median of these three values was used for further data analysis. The TBF measurement apparatus was calibrated to 250 PU in a "motility standard" reference solution (Perimed) before the measurements, and calibration was regularly confirmed. Calibration was stable over time.

Quantification of Liporubicin Distribution in Tumor and Lung Tissues

Harvested lungs were embedded in cryogenic embedding medium (OCT), sectioned, and visualized using an epifluorescence microscope to determine doxorubicin signal as previously described [13]. For each lung, a series of four red green blue (RGB) images in the tumor and in the normal lung was performed using a mercury lamp coupled to a 580-nm absorbance filter. This allowed visualizing the distribution of doxorubicin, the basic component of Liporubicin that is encapsulated in liposomes. Hereafter and throughout the text, Liporubicin quantification refers to doxorubicin signal quantification as this is the active component at the cellular level of Liporubicin. To determine the distribution of Liporubicin in the tumor, a custom-built macro for ImageJ was used as previously described [13]. Briefly, the RGB images were created, taking highly intense green images that corresponded to endothelial cell lining (red pseudocolor) and lower intense signal (green pseudocolor, Liporubicin). The dilation function was applied to the red pseudocolor image for sequential dilations. A new RGB image was recreated, and the overlap between green and red channels was quantified using the RGB colocalization function in ImageJ that quantifies the overlapped green and red pixels. This signal was corrected for initial overlap and background pixel count on the nondilated image and divided by the number of vessels per image (cross-checked by conventional histology). The results represent the presence of Liporubicin pixels as a function of distance from vessels in the different treatment groups, in other words, its distribution within tumors.

Statistical Analysis

Liporubicin signal at increasing distances from tumor vessels was assessed using a Student's *t* test in Excel (Microsoft Corporation,

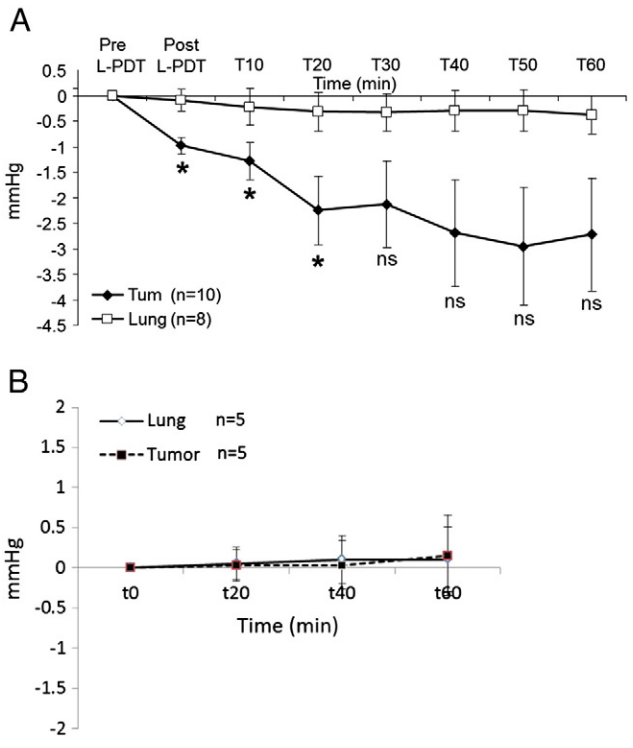

Figure 1. (A) Impact of L-PDT on tumor and lung IFP. The chart represents the changes in IFP before (30 minutes before L-PDT), during, and 1 hour after L-PDT in tumors and normal lung in sarcoma metastasis to rodent lungs (mean ± SEM; $*P < .05$ between initial and given time points, time in minutes). (B) Changes in tumor and lung IFP with only Visudyne and Liporubicin injection (no L-PDT) for 1 hour are shown.

Redmound, WA, USA) where a bidirectional hypothesis was applied. IFP and TBF changes were compared to initial values using a paired *t* test and between time points using a Student's *t* test where a bidirectional hypothesis was applied. Results were considered significant when $P < .05$.)

Results

Tumor IFP Changes with L-PDT

Before L-PDT treatment, tumor IFP values were significantly higher than lung values (4 ± 1.5 mm Hg *vs* 0 ± 0.25 mm Hg, respectively; $P < .05$). To exclude hemodynamic instability caused by anesthesia, we determined continuous tumor and lung IFP values during the first 30 minutes following anesthesia induction (Figure 1*A*, pre–L-PDT). IFP values remained constant throughout this time frame. IFP was then measured in a constant way during and up to 1 hour following L-PDT. L-PDT caused a persistent decrease in tumors but not lung IFP (Figure 1*A*) that was significantly lower than the pre–L-PDT values up to 30 minutes following light delivery. Between 30 and 60 minutes following L-PDT, tumor IFP was lower than the pre–L-PDT values, but this difference was not significant. Interestingly, tumor and lung IFP levels were not affected by Visudyne or Liporubicin administration in the five control animals when no light was administered (Figure 1*B*).

Tumor Laser Doppler Flowmetry with L-PDT

We then determined the effect of L-PDT on TBF by performing laser Doppler flowmetry. Because of the continuous ventilation, lung Doppler flowmetry was not possible as the ventilated lung caused many artifacts. Because the tumor tissue was thicker and more compact, TBF assessment in tumors was feasible and reproducible. The mean value of TBF after stabilization was of 493 ± 38 PU. L-PDT caused a brief decrease in TBF to 352 ± 46 PU in the immediate post–L-PDT period. The tumor L-PDT values recovered to pre–L-PDT values within 10 minutes following L-PDT. These values remained constant throughout the 60 minutes of the experiment (Figure 2).

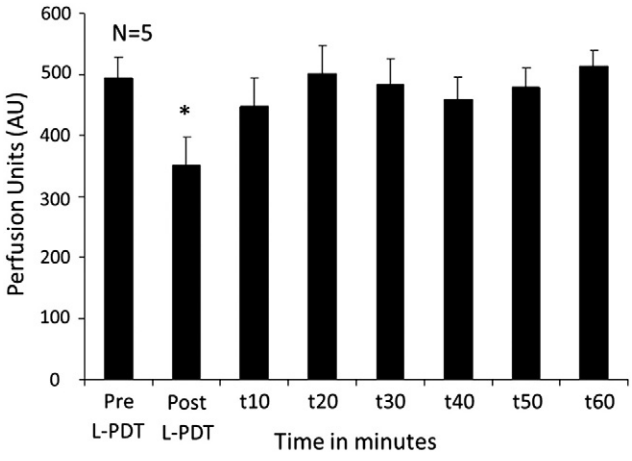

Figure 2. Laser Doppler flowmetry assessment of TBF before, during, and after L-PDT (in arbitrary PU) in sarcoma tumors generated on rodent lungs. There is a significant drop in TBF during L-PDT that recovers 10 minutes after L-PDT (mean ± SEM; *$P < .05$ between initial and current time points, time in minutes).

Liporubicin Assessed by Fluorescence Microscopy

To determine the spatial distribution of Liporubicin in tumors following IV administration, we quantified Liporubicin signal in tumor sections by epifluorescence microscopy (Figure 3, *A* and *B*). Liporubicin consists of doxorubicin encapsulated in liposomes. Doxorubicin has intrinsic fluorescent properties with an emission signal that can be recorded at an emission of 580 nm when excited by a mercury lamp. In animals treated with IV alone, doxorubicin signal was confined to the vascular area at the periphery of the tumor with a very sparse signal observable in the tumor interstitium. In tumors pretreated by L-PDT, however, the doxorubicin signal was increased and more homogenous throughout the tumor interstitium (Figure 3*A*). Signal quantification showed that L-PDT significantly enhanced the penetration depth of doxorubicin from the tumor vessels compared to IV alone ($P < .05$). In addition, the total count of pixels within the first 105 μm around tumor vessels was significantly higher in the L-PDT compared to the IV-alone group. These date suggested an enhanced and more homogenous availability of the drug within the tumors after L-PDT (Figure 3*B*).

Discussion

Photodynamic therapy was shown to induce a variety of effects ranging from transient changes in the tumor vasculature to direct tumor cytotoxic effects. A recent concept where PDT is applied at low drug/light conditions was shown to specifically affect the tumor but not normal vasculature [12,13]. These studies have shown that L-PDT of the tumor vasculature could significantly enhance the distribution of drugs administered subsequently without affecting its distribution in normal tissue [7,8]. The precise mechanism of L-PDT is still unknown as this concept is relatively new. In prostate cancer, vascular-targeted PDT was shown to enhance effective permeability of tumor vessels [15]. This was hypothesized to occur through the contraction of endothelial cells on the basis of *in vitro* results [15]. The same mechanism has also been suggested in a separate study on heterotopic colic cancer [8]. This was based on effective permeability assessments by studying the distribution of increasing fluorescent bead sizes before and after L-PDT. Interestingly, it is also known that effective permeability or molecule distribution do not necessarily correspond to the intrinsic vessel permeability. For example, it was well demonstrated that solid tumors have wide networks of neovessels that are very permeable and cause IFP to be high [16]. In addition, studies on antiangiogenic therapy have demonstrated that limiting vessel intrinsic permeability could decrease IFP, enhance convection between the intravascular and extravascular spaces, and enhance drug distribution or effective permeability of molecules in tumors as long as the drugs, such as Liporubicin, have a diameter below or equal to 100 nm [4,11]. In this study, we found that L-PDT decreased tumor but not lung IFP and had no effect on TBF (Figure 4*A*). This resulted in an enhancement of Liporubicin distribution in tumors. If we consider the IFP changes induced by L-PDT and postulate that the constant TBF, following L-PDT, suggests a stable intravascular hydrostatic pressure, the application of the Starling equation in our model predicts that L-PDT enhanced drug convection between the intravascular and extravascular spaces (Figure 4*B*). Moreover, because neovessels are highly permeable, it seems very unlikely that endothelial cell contraction and tumor vascular permeability increase could explain the observed decrease of tumor IFP in our model. Instead, our data seem to suggest that L-PDT decreases tumor vessel permeability, which reduces tumor IFP while keeping intravascular

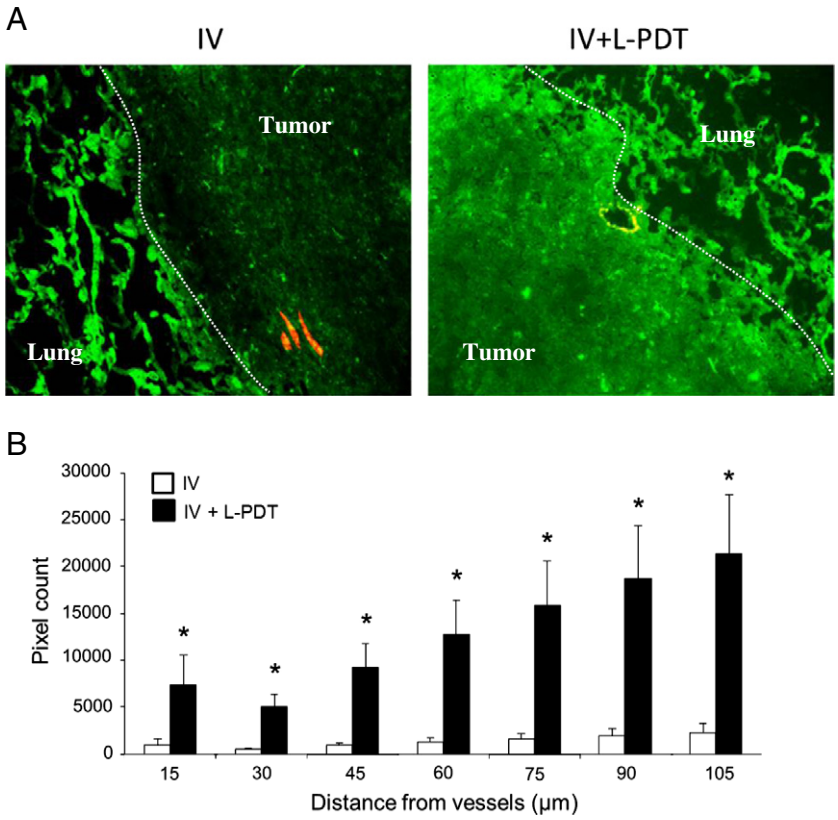

Figure 3. (A) Liporubicin fluorescence reconstruction images in tumors after administration of 400 μg of Liporubicin with and without L-PDT pretreatment (original magnification, $\times$40). The green pseudocolor represents Liporubicin signaling, and the red pseudocolor represents tumor blood vessels. L-PDT pretreatment enhanced the distribution of Liporubicin in the tumor interstitium but not in lung tissues. (B) Liporubicin signaling quantification in the tumor at increasing distances (μm) from the tumor vessels with and without L-PDT pretreatment is shown.

hydrostatic pressure stable and leaving normal tissues unaffected (Figure 4*B*). Further work to determine vessel pore size in L-PDT–treated vessels and controls by electron microscopy are necessary for proper validation of this hypothesis. A similar mechanism has been demonstrated in solid tumors treated with low doses of antiangiogenic therapy. These studies have shown that the decrease in vessel permeability decreased IFP and enhanced convection between the intravascular and extravascular spaces. These changes were named "vessel normalization" [4–11]. Separate studies showed that the decrease in vessel permeability enhanced drug distribution for drug sizes up to 100 nm in diameter [16]. Our results seem to indicate that L-PDT caused a drop in IFP through a drop in vessel permeability. However, as in normalization, tumor vessel permeability did not reach that of normal vessels [4–11]. In other words, L-PDT–treated tumor vessels had more convection and kept a certain degree of permeability that favored liporubicin extravasation and distribution.

An important topic for chemotherapy specificity and efficacy is to specifically accumulate in tumors while leaving normal tissues unaffected. In the literature, many approaches have been suggested to obtain a specific drug distribution in tumors. It was well demonstrated that tumor vessels and normal vessels are different in their structure and function. For example, the big vessel gaps in tumors that are absent in normal vessels were the basis of macromolecule (i.e., liposome) encapsulation of chemotherapy to enhance tumor drug specificity [17]. Here, we find that L-PDT administered with the drug/light conditions used has a specific effect on the tumor vasculature while leaving normal vessels unaffected. Previous studies have already suggested that the mechanism for drug distribution enhancement by L-PDT is different in normal and tumor tissues. In normal tissues, it was shown that the light irradiation conditions required for enhanced drug distribution were 10-fold higher than those necessary in tumor tissues [13,18,19]. In addition, it was demonstrated that selectins and the immune system played an important role for drug distribution enhancement in normal tissue, whereas this was not the case in tumor tissues [18,19]. The different L-PDT drug/light conditions for tumor *versus* normal tissue drug enhancement conditions could therefore be explained by different mechanisms for drug distribution occurring in normal and tumor tissues. For example, the contraction of endothelial cells and enhancement of vessel permeability in normal tissue are expected to improve drug distribution as IFP is low in normal tissues (i.e., the basis of an inflammatory reaction) but is not expected to affect tumor drug distribution (IFP is already high). In addition, differences in microarchitecture of the vasculature between normal and tumor tissues could explain the difference in sensitivity of the different vasculatures [20]. For example, low pericyte coverage is a well-known characteristic of tumor vessels [20]. Normal vessels, on the contrary, have a preserved architecture with excellent alignment of endothelial cells and pericytes [20]. Further work on the vessel architecture and

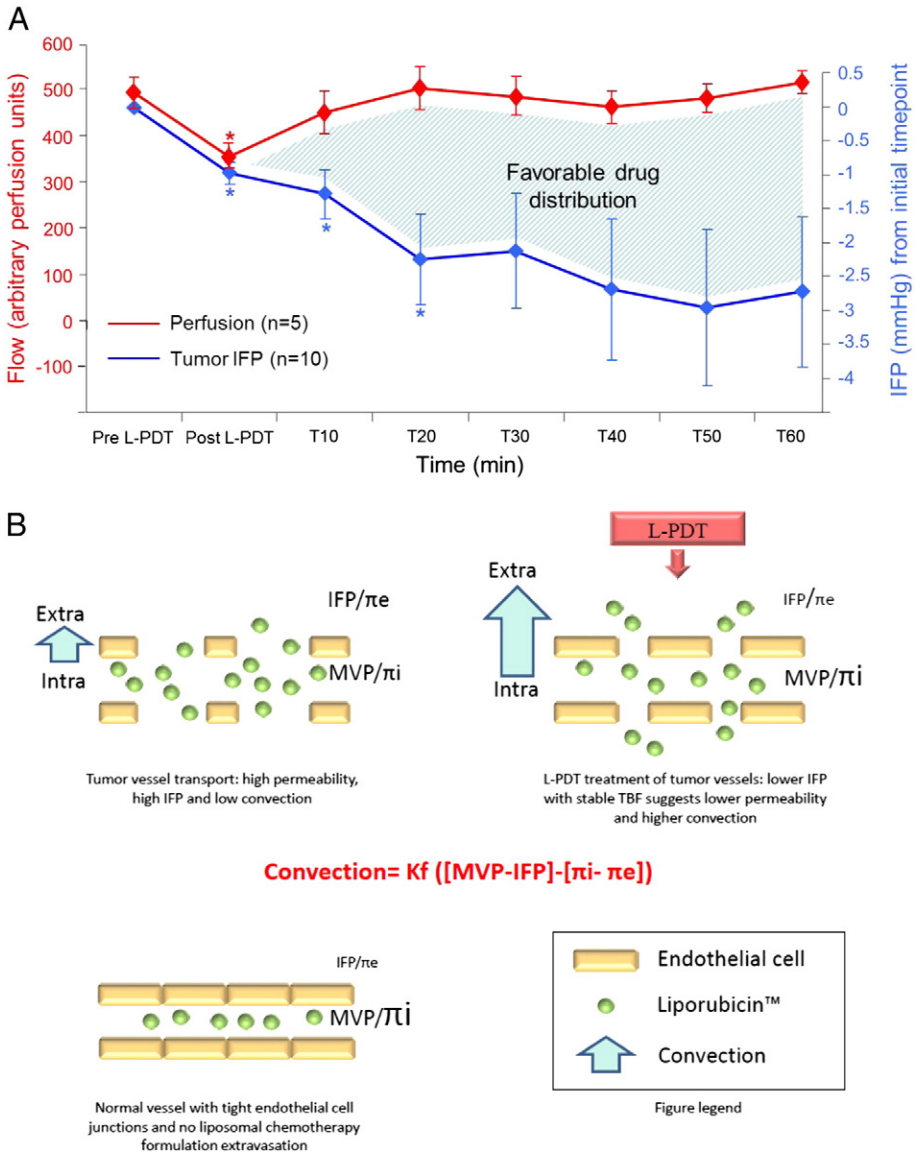

Figure 4. (A) Combination of Figures 1 and 2 shows a favorable drug distribution period ranging from before L-PDT to 60 minutes after L-PDT. (B) Schematic representation of the Starling equation parameters in solid tumors before and after L-PDT. In the pre–L-PDT condition, tumor vascular intrinsic permeability is increased. This causes oncotic pressures to equilibrate between the intravascular and extravascular spaces (πi: oncotic capillary pressure; πe: oncotic IFP). This also causes the hydrostatic IFP to be high. L-PDT is thought to induce a change in vascular permeability that decreases IFP and recreates an oncotic gradient between the intravascular and extravascular space between 10 and 60 minutes following L-PDT. According to the Starling equation, convection is increased after L-PDT compared to the initial time point (light blue arrow line). As a comparison, a normal vessel is also represented with tight endothelial cell junctions that impair macromolecule extravasation.

changes with L-PDT is required to determine the mechanism responsible for permeability changes in tumor vessels.

The effect of photodynamic therapy on tumor IFP has been studied in the past. Interestingly, the drug/light conditions used were higher than in the present study and aimed to cause tumor cytostatism. Dolmans and collaborators, for example, had shown in MCA4 mammary tumors that photodynamic therapy caused a transient vasospasm that was followed after 4 hours by vessel permeability increase [21]. This was also the case in melanomas grown on hamsters where cytostatic photodynamic therapy caused a two-phase response with an acute permeability of tumor vessels, followed by a drop in IFP after 24 hours because of vascular shutdown [22]. It thus appears that phototherapy can have multiple and long-term effects on the tumor vasculature that are not only confined to the treatment period. This could be of interest in situations of repeated chemotherapy administration schemes for clinical translation in patients. In this study, we chose to only study the short-term effect of L-PDT on IFP and TBF as chemotherapy was administered once, and its distribution was assessed after 1 hour. It is mandatory to further determine how L-PDT affects the tumor and normal vasculatures for longer periods of time and how this affects subsequent administrations of chemotherapy. In addition, these observations further underline the need to obtain specific biomarkers for L-PDT assessment in patients to better optimize treatments.

A clinical translation of our study in patients, although the procedure remains complex and invasive, could be of interest in superficially spreading tumors such as mesotheliomas or oligometastatic pleural disseminations. Indeed, this therapy has limited side effects and an important effect on drug distribution enhancement. However, optimal drug/light conditions are mandatory for tumor blood vessel L-PDT to be successful. Therefore, a better understanding of how photosensitization modifies the vascular function and refinements of *in situ* L-PDT monitoring are mandatory for the translation of this concept in a clinical setting. Few parameters currently exist to assess the impact of L-PDT on the vasculature and thus determine the appropriate sequence of administration of chemotherapy following L-PDT for best therapeutic results. On the basis of our study, we find two promising factors, IFP and TBF, that could be translated in the clinics after validation to monitor the effect of L-PDT on solid tumors. The application of L-PDT in combination with chemotherapy could thus be performed using the wick-in-needle technique *in vivo* with laser Doppler flowmetry to monitor and confirm the vascular effect of L-PDT. Therefore, IFP and TBF could represent two potential biomarkers that could be used for L-PDT translation in the clinics. Other biomarkers such as circulation angiogenic factors over time and imaging of vessel permeability by Magnetic Resonnance Imaging (MRI), for example, should also be exploited. These elements have shown robustness in clinical trials combining antiangiogenic therapy with chemotherapy in the aim to optimize the normalization concept. In the L-PDT field, no studies have so far been performed with this concept. These elements therefore require validation but could be of interest to translate L-PDT in the clinics.

In conclusion, Visudyne-mediated L-PDT has the potential to selectively enhance Liporubicin distribution in tumors in a model of sarcoma metastasis to the lung by reducing tumor IFP. The enhancement of convection in tumors by L-PDT is a novel and attractive concept that opens new perspectives for the management of superficially spreading tumors.

Acknowledgments

We are grateful to N. Lange for his critical review of the manuscript.

References

[1] Jain RK and Eugene M (1997). The Landis Award Lecture 1996. Delivery of molecular and cellular medicine to solid tumors. *Microcirculation* **4**(1), 1–23.

[2] Jain RK (2005). Normalization of tumor vasculature: an emerging concept in antiangiogenic therapy. *Science* **307**(5706), 58–62.

[3] Krueger T, Kuemmerle A, Andrejevic-Blant S, Yan H, Pan Y, Ballini JP, Klepetko W, Decosterd LA, Stupp R, and Ris HB (2006). Antegrade *versus* retrograde isolated lung perfusion: doxorubicin uptake and distribution in a sarcoma model. *Ann Thorac Surg* **82**(6), 2024–2030.

[4] Tong RT, Boucher Y, Kozin SV, Winkler F, Hicklin DJ, and Jain RK (2004). Vascular normalization by vascular endothelial growth factor receptor 2 blockade induces a pressure gradient across the vasculature and improves drug penetration in tumors. *Cancer Res* **64**(11), 3731–3736.

[5] Yan H, Cheng C, Haouala A, Krueger T, Ballini JP, Peters S, Decosterd LA, Letovanec I, Ris HB, and Andrejevic-Blant S (2008). Distribution of free and liposomal doxorubicin after isolated lung perfusion in a sarcoma model. *Ann Thorac Surg* **85**(4), 1225–1232.

[6] Shirasu N, Nam SO, and Kuroki M (2013). Tumor-targeted photodynamic therapy. *Anticancer Res* **33**(7), 2823–2831.

[7] Cheng C, Debefve E, Haouala A, Andrejevic-Blant S, Krueger T, Ballini JP, Peters S, Decosterd L, van den Bergh H, and Wagnieres G, et al (2010). Photodynamic therapy selectively enhances liposomal doxorubicin uptake in sarcoma tumors to rodent lungs. *Lasers Surg Med* **42**(5), 391–399.

[8] Snyder JW, Greco WR, Bellnier DA, Vaughan L, and Henderson BW (2003). Photodynamic therapy: a means to enhanced drug delivery to tumors. *Cancer Res* **63**(23), 8126–8131.

[9] Chen B, Crane C, He C, Gondek D, Agharkar P, Savellano MD, Hoopes PJ, and Pogue BW (2008). Disparity between prostate tumor interior *versus* peripheral vasculature in response to verteporfin-mediated vascular-targeting therapy. *Int J Cancer* **123**(3), 695–701.

[10] Wang Y, Gonzalez M, Cheng C, Haouala A, Krueger T, Peters S, Decosterd LA, van den Bergh H, Perentes JY, and Ris HB, et al (2012). Photodynamic induced uptake of liposomal doxorubicin to rat lung tumors parallels tumor vascular density. *Lasers Surg Med* **44**(4), 318–324.

[11] Chauhan VP, Stylianopoulos T, Martin JD, Popović Z, Chen O, Kamoun WS, Bawendi MG, Fukumura D, and Jain RK (2012). Normalization of tumour blood vessels improves the delivery of nanomedicines in a size-dependent manner. *Nat Nanotechnol* **7**(6), 383–388.

[12] Cheng C, Haouala A, Krueger T, Mithieux F, Perentes JY, Peters S, Decosterd LA, and Ris HB (2009). Drug uptake in a rodent sarcoma model after intravenous injection or isolated lung perfusion of free/liposomal doxorubicin. *Interact Cardiovasc Thorac Surg* **8**(6), 635–638.

[13] Cheng C, Wang Y, Haouala A, Debefve E, Andrejevic Blant S, Krueger T, Gonzalez M, Ballini JP, Peters S, and Decosterd L, et al (2011). Photodynamic therapy enhances liposomal doxorubicin distribution in tumors during isolated perfusion of rodent lungs. *Eur Surg Res* **47**(4), 196–204.

[14] Ley CD, Horsman MR, and Kristjansen PE (2007). Early effects of combretastatin-A4 disodium phosphate on tumor perfusion and interstitial fluid pressure. *Neoplasia* **9**(2), 108–112.

[15] Chen B, Pogue BW, Zhou X, O'Hara JA, Solban N, Demidenko E, Hoopes PJ, and Hasan T (2005). Effect of tumor host microenvironment on photodynamic therapy in a rat prostate tumor model. *Clin Cancer Res* **11**(2 Pt 1), 720–727.

[16] Fukumura D, Duda DG, Munn LL, and Jain RK (2010). Tumor microvasculature and microenvironment: novel insights through intravital imaging in pre-clinical models. *Microcirculation* **17**(3), 206–225.

[17] Milla P, Dosio F, and Cattel L (2012). PEGylation of proteins and liposomes: a powerful and flexible strategy to improve the drug delivery. *Curr Drug Metab* **13**(1), 105–119.

[18] Debefve E, Cheng C, Schaefer SC, Yan H, Ballini JP, van den Bergh H, Lehr HA, Ruffieux C, Ris HB, and Krueger T (2010). Photodynamic therapy induces selective extravasation of macromolecules: insights using intravital microscopy. *J Photochem Photobiol B* **98**(1), 69–76.

[19] Debefve E, Mithieux F, Perentes JY, Wang Y, Cheng C, Schaefer SC, Ruffieux C, Ballini JP, Gonzalez M, and van den Bergh H, et al (2011). Leukocyte-endothelial cell interaction is necessary for photodynamic therapy induced vascular permeabilization. *Lasers Surg Med* **43**(7), 696–704.

[20] Goel S, Duda DG, Xu L, Munn LL, Boucher Y, Fukumura D, and Jain RK (2011). Normalization of the vasculature for treatment of cancer and other diseases. *Physiol Rev* **91**(3), 1071–1121.

[21] Dolmans DE, Kadambi A, Hill JS, Flores KR, Gerber JN, Walker JP, Borel Rinkes IH, Jain RK, and Fukumura D (2002). Targeting tumor vasculature and cancer cells in orthotopic breast tumor by fractionated photosensitizer dosing photodynamic therapy. *Cancer Res* **62**(15), 4289–4294.

[22] Leunig M, Goetz AE, Gamarra F, Zetterer G, Messmer K, and Jain RK (1994). Photodynamic therapy-induced alterations in interstitial fluid pressure, volume and water content of an amelanotic melanoma in the hamster. *Br J Cancer* **69**(1), 101–103.